


Emergence of a spin-liquid-like phase in the quantum spin ladder compound $\text{Ba}_2\text{CuTeO}_6$ with chemical substitution

Shalini Badola ^{*}, Devesh Negi , Aprajita Joshi , Asif Ali , Ravi Shankar Singh , and Surajit Saha [†]
Indian Institute of Science Education and Research Bhopal, Bhopal 462066, India

 (Received 21 September 2023; revised 23 February 2024; accepted 28 February 2024; published 20 March 2024)

The stabilization of quantum spin liquids is vital to realize applications in spintronics and quantum computing. The unique magnetic structure of $\text{Ba}_2\text{CuTeO}_6$ comprising coupled spin ladders with finite interladder coupling brings the system close to the quantum critical point. This opens up possibilities to stabilize unconventional magnetic phases by tailoring the intra- and interladder exchange couplings. Here, we demonstrate a spin-liquid-like phase in $\text{Ba}_2\text{CuTeO}_6$ using the method of chemical substitution. We choose nonmagnetic La^{3+} cation to substitute the Ba^{2+} in $\text{Ba}_2\text{CuTeO}_6$ and present signature fingerprints such as a deprived magnetic transition, nondispersive ac susceptibility, magnetic-field-independent heat capacity, and a broad Raman continuum supporting the emergence of a spin-liquid-like phase. We believe that increased magnetic frustration and spin fractionalization upon chemical substitution play a crucial role in driving such a state. In addition, temperature and magnetic-field-dependent phonon responses indicate the presence of magnetostriction (spin-lattice coupling) in La-doped $\text{Ba}_2\text{CuTeO}_6$, a notable property of spin liquids.

DOI: [10.1103/PhysRevB.109.L100405](https://doi.org/10.1103/PhysRevB.109.L100405)

Spin systems with quantum criticalities hold great potential to exhibit unconventional ground states such as spin liquids. Quantum spin systems are materials that generally avoid magnetic ordering as a consequence of dominant quantum spin fluctuations. Anderson proposed the notion of enhanced quantum fluctuations in low-spin candidates, particularly the $S = \frac{1}{2}$ and 1 compounds, systems with low-spin connectivity, and frustrated bond networks [1]. The complex interplay between the growing fluctuations (both thermal and spin) and exchange interactions leads to novel ground states in condensed matter systems with a strong relevance in spintronics, quantum computing, etc. The novel states have been understood in low-spin cuprates as well as highly spin-orbit-coupled iridates with the realization of weak antiferromagnets, spin liquids, resonance valence bond states along with fractionalized excitations, and unconventional superconductivity [1–4]. In particular, $S = \frac{1}{2}$ systems forming spin chains, triangular, and ladder-like spin structures are host to unusual fractionalized excitations, leading to quantum spin liquids. However, these states are rare and challenging to stabilize because of a delicate balance between the thermodynamics and disorder. Therefore, low-spin candidates with weak spin connectivity are promising test-beds to stabilize these new exotic phases.

Spin ladder $\text{Ba}_2\text{CuTeO}_6$, which lies in the extreme quantum regime of low spin ($S = \frac{1}{2}$) and weak bond networks, has recently drawn enormous interest of the community [5]. The electronic degeneracy of the Cu^{2+} cation in CuO_6 octahedra leads to the Jahn-Teller effect which in turn promotes low magnetic dimensionality in the system. In contrast, TeO_6 exhibits a strong tendency to build a three-dimensional (3D)

network. In this conflicting scenario, due to the interladder coupling, the system exists close to the quantum critical point. Previous reports suggest that $\text{Ba}_2\text{CuTeO}_6$ exhibits a crossover in magnetic dimensionality from the paramagnetic phase to a short-ranged quasi-two-dimensional (2D) spin ladder state below ~ 75 K and then to a (3D) antiferromagnetic state below ~ 15 K [see Fig. 1(a)] [6,7]. The ladder state, which is the intermediate state, exists in the bc plane with interladder interactions along the c direction [refer to Fig. 1(b)]. The finite leg (J_l) and rung (J_r) interactions ($J_l/J_r \neq 0$) along with weak interladder coupling extend beyond the two-leg limit, thus stabilizing a 3D ordered antiferromagnetic network below ~ 15 K. Theory and experiments have established that even-leg ladder systems may exhibit a spin-liquid state with exponentially decaying spin-spin correlations (SSCs) [8,9]. On the other hand, odd-leg ladders behave similar to spin chain systems with power-law decay SSCs [8]. In fact, indications of a possible spin-liquid-like state have been suggested in $\text{Ba}_2\text{CuTeO}_6$ using the electron spin resonance (ESR) technique but in the intermediate spin ladder state only [7]. $\text{Ba}_2\text{CuTeO}_6$ consists of a dominant two-leg spin ladder network with weak interladder coupling. Tailoring the intra- and interladder couplings in $\text{Ba}_2\text{CuTeO}_6$ can therefore introduce uncompensated interactions in the spin lattice, thereby evolving the quasi-2D magnetic character into such unconventional phases.

Chemical substitution is an effective approach to tailor the exchange interactions and establish unconventional but novel phases in condensed matter systems [10,11]. The decoupling of ladders and evolution of magnetic properties was recently demonstrated by Pughe *et al.* in $\text{Ba}_2\text{CuTeO}_6$ with a chemical substitution [12]. With this motivation, herein, we demonstrate that a quantum spin-liquid-like state can be realized in $\text{Ba}_2\text{CuTeO}_6$ through the chemical substitution

^{*}badolasha20@gmail.com

[†]surajit@iiserb.ac.in

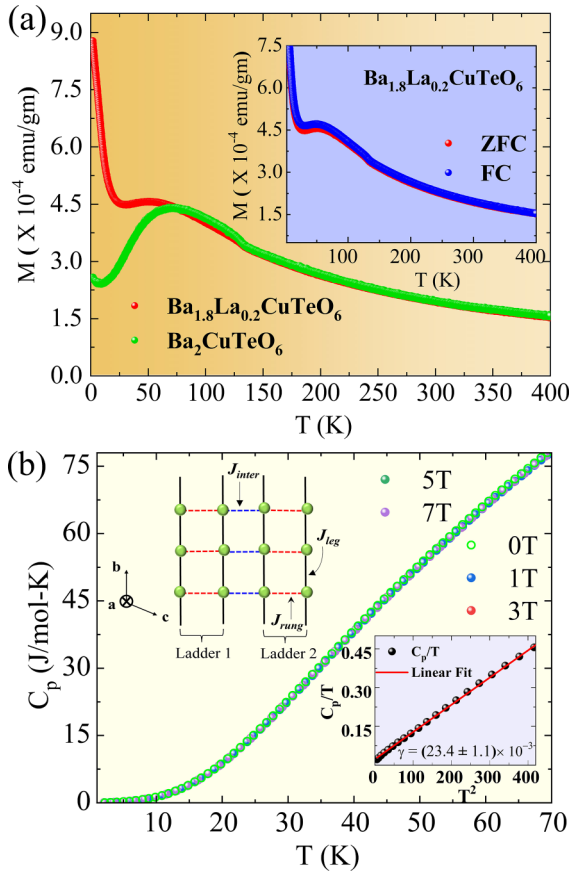


FIG. 1. (a) Magnetic susceptibility of the $\text{Ba}_2\text{CuTeO}_6$ and $\text{Ba}_{1.8}\text{La}_{0.2}\text{CuTeO}_6$. The inset shows that ZFC and FC curves of $\text{Ba}_{1.8}\text{La}_{0.2}\text{CuTeO}_6$ coincide at all temperatures. (b) Specific heat capacity shown as a function of temperature at variable magnetic fields. The inset displays a linear fit to $C_p/T = \gamma + \beta T^2$.

of Ba^{2+} by La^{3+} with a possible charge compensation of Cu^{2+} , consequently breaking the spin pairs in the spin ladder. The observed signatures of the spin-liquid phase are (i) the suppression of magnetic transition and the presence of a nondispersive magnetic susceptibility in a doped system, (ii) a magnetic-field-independent heat capacity along with the signatures of fermionic density of states, and (iii) the two-magnon (2M) feature in the Raman spectrum of $\text{Ba}_2\text{CuTeO}_6$ turning into a broad continuum in La-doped $\text{Ba}_2\text{CuTeO}_6$ at 5 K. The observed spin-liquid-like behavior in La-doped $\text{Ba}_2\text{CuTeO}_6$ may originate from the fractionalization of spin singlets and/or an increased magnetic frustration upon chemical substitution, which is also tested using other isoelectronic dopings such as Ni^{2+} and Zn^{2+} but at the B site (Cu site). Moreover, we observe anomalies in the phonon behavior with temperature and magnetic field in doped $\text{Ba}_2\text{CuTeO}_6$ that are attributed to spin-phonon (spin-lattice) coupling, which are also notable characteristics of spin liquids.

Present investigations have been carried out on pelletized polycrystalline samples of $\text{Ba}_{1.9}\text{La}_{0.1}\text{CuTeO}_6$, $\text{Ba}_{1.8}\text{La}_{0.2}\text{CuTeO}_6$ (BLCT), $\text{Ba}_{1.7}\text{La}_{0.3}\text{CuTeO}_6$, $\text{Ba}_2\text{CuTeO}_6$ (BCT), $\text{Ba}_2\text{Cu}_{0.8}\text{Zn}_{0.2}\text{TeO}_6$ (BCZT), and $\text{Ba}_2\text{Cu}_{0.9}\text{Ni}_{0.1}\text{TeO}_6$ (BCNT) synthesized using the solid-state reaction method at temperatures of 750, 900, and 1050 °C, respectively.

The room-temperature x-ray diffraction profiles of BCT, BLCT, and other La-doped BCT systems, recorded with a PANalytical x-ray diffractometer, are analyzed using Rietveld refinement and are presented in the Supplemental Material (refer to Fig. S1) [13]. The lattice parameters of the systems suggest the stabilization of the triclinic phase (space group $P\bar{1}$). A further analysis is included in the Supplemental Material [13–16]. A Rietveld analysis detects a minor fraction ($\sim 1.9\%$) of the secondary phase of precursor La_2O_3 in the doped system BLCT, which seemingly does not impair the magnetism and the other measured properties. Notably, the structural symmetry of BLCT/BCNT/BCZT remains unaltered at room temperature despite the substitution of larger divalent Ba^{2+} with a smaller trivalent La^{3+} ion. The successful incorporation of $\text{La}^{3+}/\text{Ni}^{2+}/\text{Zn}^{2+}$ ions into the BCT matrix is confirmed using x-ray diffraction. Energy-dispersive x-ray spectroscopy was employed to confirm sample stoichiometry, the details of which are provided in the Supplemental Material [13].

Figure 1(a) presents the temperature-dependent dc magnetization of the parent and La-doped system (BCT and BLCT, respectively) recorded using a Quantum Design superconducting quantum interference device vibrating sample magnetometer (SQUID-VSM) setup. The magnetization of BCT displays a broad feature peaking at $T_S \sim 75$ K, a property common to low-dimensional antiferromagnets, depicting the presence of short-ranged spin correlations. The broad feature in magnetization intriguingly undergoes a suppression and shifts toward lower temperature upon doping La^{3+} at the Ba^{2+} site (in BLCT) avoiding any discernible spin ordering down to the lowest temperature (2 K) measured, as shown in Fig. 1(a). It is to be noted that La^{3+} is a nonmagnetic ion and is not expected to alter the magnetism of BCT so significantly upon doping, yet a smaller size and distinct oxidation of La^{3+} may change the local bond parameters and contribute uncompensated spin interactions to the lattice due to a charge disparity at the Ba site, influencing its magnetic behavior through a modification of the exchange pathways. A decrease in the magnetic moment may be noted from $(1.8483 \pm 0.0003)\mu_B$ for BCT to $(1.8191 \pm 0.0009)\mu_B$ for BLCT (see Supplemental Material [13]). Although there is a small change in the magnetic moment, it may be due to the conversion of Cu^{2+} into Cu^+ by a small fraction to maintain the charge neutrality of the system as evidenced from x-ray photoelectron spectroscopy (see Supplemental Material [13]) [17–19]. Furthermore, the magnetization of the BLCT exhibits a paramagnetic behavior below $T_p \sim 20$ K which is very weak in the parent system BCT [see Fig. 1(a)]. The inset in Fig. 1(a) shows that the magnetization data recorded under zero-field-cooled (ZFC) and field-cooled (FC) protocols for BLCT reveal no sizable bifurcation in the temperature range under investigation, ruling out the existence of a spin-glass phase [20]. This is further corroborated by the ac magnetic susceptibility (χ' the real part and χ'' the imaginary part) measurements which revealed a nondispersive χ' upon varying the frequency of the applied magnetic field (refer to Fig. S2 in the Supplemental Material [13]). Moreover, χ'' also remained close to zero, showing a negligible change under the variable frequency of the applied magnetic field. All of these findings in BLCT are suggestive of a potential spin-liquid behavior and therefore

call for further measurements to fully understand the distinct characteristics observed in our magnetic studies.

Heat capacity and inelastic light scattering have been two extremely efficient probes to elucidate the nature of spin-spin correlations and their evolution with temperature (T) and magnetic field [21–24]. We performed heat capacity and Raman measurements on polycrystalline BCT and BLCT with varying temperatures and magnetic fields (see Supplemental Material [13]). The heat capacity, measured using a physical property measurement system (PPMS), reveals that BLCT does not exhibit a sharp λ -like anomaly [see Fig. 1(b)], signifying the absence of any long-ranged spin-ordered state down to 2 K. Note that even BCT does not show a clear signature of long-range ordering. As shown in Fig. 1(b), the C_p vs T for BLCT exhibits a behavior that is independent of applied magnetic field, thus confirming the absence of a spin-glass phase, as also suggested from our static (dc) and dynamic (ac) magnetic measurements. The heat capacity of BLCT is fitted with $C_p/T = \gamma + \beta T^2$ at low temperatures ($2 \text{ K} < T < 20 \text{ K}$) yielding $\gamma = 23.4 \pm 1.1 \text{ mJ mol}^{-1} \text{ K}^{-2}$ and $\beta = 1.05 \pm 0.01 \text{ mJ mol}^{-1} \text{ K}^{-4}$ [see the inset in Fig. 1(b)]. A large magnitude of γ (typically in between 1 and 250 $\text{mJ mol}^{-1} \text{ K}^{-2}$) in doped BLCT is indicative of a contribution from the fermionic density of states (DOS) [20,25]. These states may arise due to quasiparticles introduced through a chemical substitution of Ba^{2+} by La^{3+} . Notably, γ does not change with varying magnetic field, thus ruling out the presence of any paramagnetic impurity [26]. The value of γ could not be estimated for BCT as the specific heat (C_p/T vs T^2) deviates from linearity below 15 K [6] (see Supplemental Material [13]). The subtle difference in C_p of BCT and BLCT at $T < 15 \text{ K}$ is suggestive of a possible subtle difference in their respective magnetic ground states.

To further understand the characteristic features discussed above, Raman measurements were performed using a LabRAM HR Evolution Raman spectrometer attached to an attoDRY 1000 He cryostat down to 4 K with an excitation laser source of wavelength 532 nm. Figure 2(a) presents a comparison of the Raman spectra of the parent system BCT and its doped variants at 5 K. The Raman spectrum of BCT demonstrates a broad feature peaking near 190 cm^{-1} which is identified as 2M excitation in an earlier work by Gibbs *et al.* [7]. On the contrary, the A -site (La^{3+}) doped analog of BCT (i.e., BLCT) reveals the existence of a broad continuum background (instead of 2M) extended in energy from 0 meV to above $\sim 40 \text{ meV}$. To understand the origin of the continuum in BLCT, the Raman spectra of other compositions but with B -site doping (Ni and Zn doping at the Cu site) in BCT (BCNT and BCZT) have been compared and are shown in Fig. 2(a). It is intriguing to note that a 2M feature, similar to that in the parent compound BCT, remained nearly unaffected and was also observed in BCNT and BCZT at energies ~ 185 and $\sim 160 \text{ cm}^{-1}$, respectively. While the substitution of magnetic (Ni^{2+}) and nonmagnetic (Zn^{2+}) ions at the B site (Cu^{2+}) does not destroy the 2M excitation, doping of a nonmagnetic ion (La^{3+}) at the A site (Ba^{2+}) transforms the 2M mode to a broad continuum. This implies a strong role of A -site substitution on the lattice. A recent report on an inelastic neutron scattering study of BCT revealed that the magnons lie in the bc plane [27] [see Fig. 1(b)]. Notably, the crystal structure

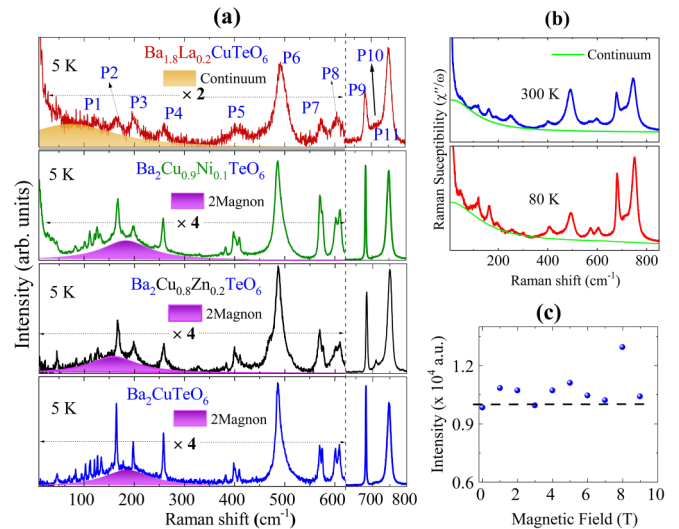


FIG. 2. (a) Raman spectrum of the parent phase $\text{Ba}_2\text{CuTeO}_6$ and doped variants $\text{Ba}_2\text{Cu}_{0.8}\text{Zn}_{0.2}\text{TeO}_6$, $\text{Ba}_2\text{Cu}_{0.9}\text{Ni}_{0.1}\text{TeO}_6$, and $\text{Ba}_{1.8}\text{La}_{0.2}\text{CuTeO}_6$ showing two-magnon (2M) and broad continuum at 5 K. Phonons are designated as P1–P11 at 5 K and the spectra are magnified in the range 10–650 cm^{-1} . (b) Temperature evolution of the low-frequency region of $\text{Ba}_{1.8}\text{La}_{0.2}\text{CuTeO}_6$ showing a broad feature (shown with a green line). (c) Magnetic-field-dependent intensity of the continuum in $\text{Ba}_{1.8}\text{La}_{0.2}\text{CuTeO}_6$.

depicts that the Ba ion (A site), where chemical substitution is made in this work, exists in between the ladder planes (along the a axis). An antisite substitution of the La ion at the Te and Cu site is highly unlikely due to a large difference in the sizes of the two ions and their oxidation states. Therefore, the origin of a broad continuum instead of the 2M mode in BLCT needs proper understanding, which is discussed below.

The presence of a broad continuum in the Raman spectrum at low temperatures is intriguing and often associated with the spin, orbital, and/or electronic fluctuations appearing over different temperature and magnetic energy scales. Some of the recent examples of such cases include a broad continuum arising due to fractionalized Majorana fermionic excitations in triangular Kitaev magnets α - RuCl_3 and $\beta(\gamma)$ - Li_2IrO_3 [2,28], antiferro- and ferro-orbitals in $\text{LaMnO}_{3+\delta}$ ($0.085 \leq \delta \leq 0.125$) [29], and intervalley fluctuations from single-particle excitations in doped Si [30]. We believe that the electronic and orbital origin of the continuum in BLCT is unlikely since its band gap is large ($\sim 1 \text{ eV}$) and an orbital contribution usually occurs at much higher-energy scales (typically observed in the range 0.25–2.5 eV), respectively [31]. The absence of a magnetic order (down to 2 K) and the existence of a broad continuum being present down to $\sim 0 \text{ meV}$ ($\sim 0 \text{ cm}^{-1}$) energy is indicative of the 2M excitation ($S = 1$) of BCT transforming into a broad spin continuum ($S \neq 1$) with La doping. The analysis of temperature and magnetic field dependence of the continuum reveals intriguing details, as shown in Figs. 2(b) and 2(c). It is observed that the continuum exists even above room temperature. It is worth noting here that such a broad Raman continuum has been reported in systems hosting Kitaev spin-liquid behavior, such as Li_2IrO_3 [2], α - RuCl_3 [28], etc., and is attributed to arise from

fractionalized Majorana excitations ($S = \frac{1}{2}$). Furthermore, our measurements show no effect of the applied magnetic field on the intensity (spectral weight) of this continuum at 5 K [see Fig. 2(c)]. Therefore, the observation of the continuum at higher temperatures and its invariance with the magnetic field are indicative of the spin-liquid-like correlations in BLCT. It is to be noted that these findings were also examined for different amounts of dopings of La at the Ba site in BCT (viz., $\text{Ba}_{1.9}\text{La}_{0.1}\text{CuTeO}_6$ and $\text{Ba}_{1.7}\text{La}_{0.3}\text{CuTeO}_6$) and were found to be consistent with our observations (see more details in the Supplemental Material [13]).

In addition, it must be noted that most of the phonon modes which appear intense and sharp in BCT have merged, becoming significantly less intense, and broadened in BLCT even at low temperatures (e.g., at 5 K), indicating a renormalization of the phonons upon chemical substitution. Among all the phonon modes of BLCT, the magnetic field (H) response of the modes P5 ($\sim 408 \text{ cm}^{-1}$), P6 ($\sim 490 \text{ cm}^{-1}$), and P8 ($\sim 608 \text{ cm}^{-1}$) are notable and shown in Fig. 3. We find that the frequency of these modes shows an increasing trend with an increasing field. Such a field dependence is absent for these phonons in the parent phase BCT (refer to the Supplemental Material [13]). A magnetic-field-dependent phonon response is suggestive of the presence of magnetostriction, i.e., a coupling between spin and lattice degrees of freedom in BLCT [32] and not seen in BCT. On the other hand, the remaining phonon modes show a very weak field dependence. Coupled spin-lattice dynamics can also be elucidated from a temperature-dependent Raman measurement which reveals that a few phonon modes, especially P5–P11 (see Fig. 3), show an anomalous trend in frequency (ω) upon decreasing the temperature by deviating from conventional cubic anharmonicity [$\Delta\omega^{\text{anh}}(T)$]. In the absence of strong magnetic, electronic, and lattice correlations, a cubic-anharmonic trend governs the phonon behavior, which is expressed as [33,34]

$$\Delta\omega^{\text{anh}}(T) = \omega_0 + A \left(1 + \frac{2}{e^{\frac{\hbar\omega}{2k_B T}} - 1} \right), \quad (1)$$

where ω_0 and A are the fitting parameters, and \hbar and k_B depict the Planck's and Boltzmann constants, respectively. On the other hand, the low-frequency phonons (P1–P4) obey standard anharmonic behavior, showing a decreasing frequency with increasing temperature.

A careful observation of Fig. 3 indicates that phonons exhibit anomalies around two temperature ranges upon cooling, first below 75 K and then below 20 K. The two temperature ranges in BLCT refer to the short-range ordered magnetic state below $T_S \sim 75 \text{ K}$ and a paramagnetic-like response below $T_P \sim 20 \text{ K}$, as observed in the magnetization data. The observed anomalies in the phonon response below 75 and 20 K can be attributed to spin-phonon coupling mediated through modulation of the exchange pathway and interaction with fractionalized excitations, as also observed in Kitaev- Cu_2IrO_3 [35].

The signatures of the quantum spin-liquid-like state obtained in magnetic, specific heat, and Raman measurements can be understood by considering two scenarios: (1) based on geometrical factors, especially the in-plane and out-of-plane Cu-Cu separations (extracted using VESTA [36]) and (2)

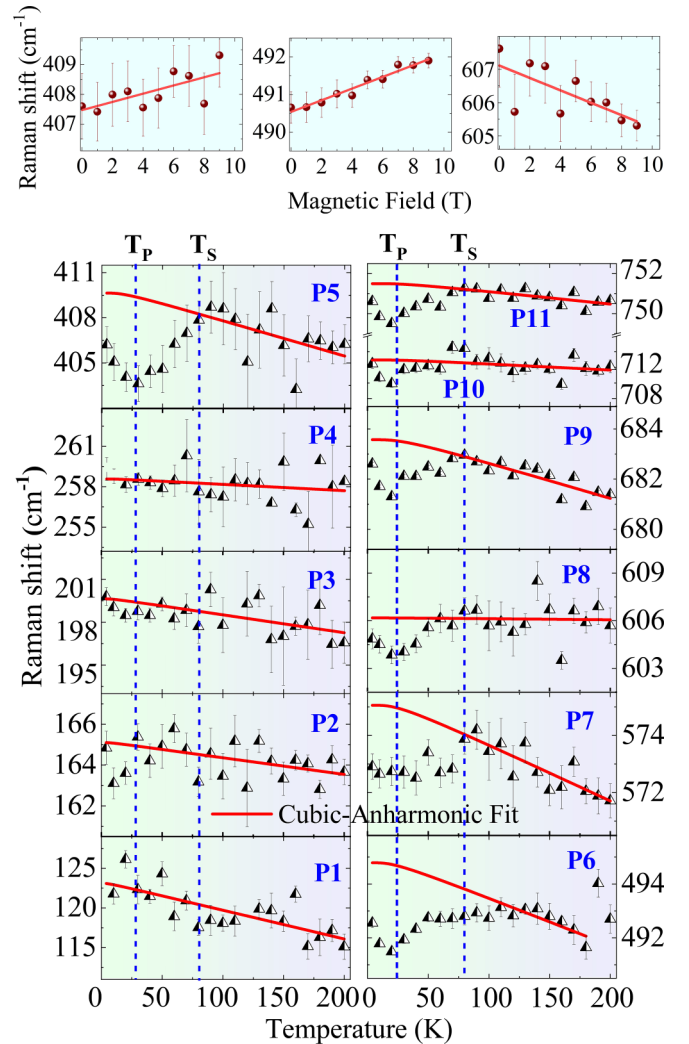


FIG. 3. Top panel: Magnetic field dependence of a few phonons. Lower panel: Phonon frequencies as a function of temperature fitted with cubic anharmonicity (solid red line). Vertical dashed lines represent the transition temperatures T_P and T_S . Error bars are included for frequencies.

conversion of Cu^{2+} ($S = \frac{1}{2}$) to Cu^+ ($S = 0$) in BLCT. In the first scenario, we observed that the Cu-Cu separation between the ladder planes (along the a axis) increases upon chemical substitution. On the contrary, the in-plane Cu-Cu separations in BLCT show decrements as compared to the parent BCT (see Fig. 4). A decreased Cu-Cu separation in the triangular spin arrangement of ladders in BLCT is likely to frustrate the spins more as evidenced in the form of a lack of magnetic order. Details of the magnetic frustration in BCT and BLCT are provided schematically in Fig. 4 and the Supplemental Material [13]. In the other scenario, an oxidation state conversion from Cu^{2+} ($S = \frac{1}{2}$) to Cu^+ ($S = 0$) in BLCT partially breaks the spin pairs due to doping by a trivalent La^{3+} at the A site. The inverse susceptibility data suggest comparable magnetic moments for the two systems (BCT: $1.84 \mu_B$ and BLCT: $1.82 \mu_B$) (see Supplemental Material [13]), implying the conversion of a small fraction of the Cu oxidation state. Even though small, unsatisfied Cu interactions due to La

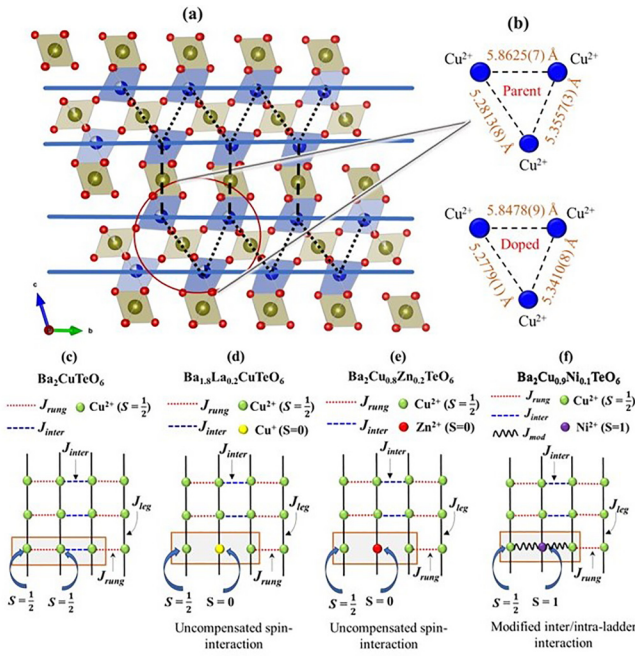


FIG. 4. (a) A schematic depiction of a spin ladder configuration in Ba_{1.8}La_{0.2}CuTeO₆ where short- and long-dashed lines refer to rung and interladder interactions, respectively. (b) Cu-Cu separations in the triangular units of spin ladders of parent Ba₂CuTeO₆ and doped Ba_{1.8}La_{0.2}CuTeO₆. Spin-spin interactions (see the enclosed rectangular box) between the ladders in (c) the parent Ba₂CuTeO₆ system and their evolution in *A/B*-site doped compositions (d) Ba_{1.8}La_{0.2}CuTeO₆, (e) Ba₂Cu_{0.8}Zn_{0.2}TeO₆, and (f) Ba₂Cu_{0.9}Ni_{0.1}TeO₆, where J_{rung} , J_{inter} , and J_{leg} depict the magnetic interactions along the rung, between, and the leg of the ladders, respectively. J_{mod} refers to the modified spin interaction in (f) Ba₂Cu_{0.9}Ni_{0.1}TeO₆.

doping will produce fractionalized quasiparticles ($S = \frac{1}{2}$) in the lattice which are formed out of broken spin-pair interactions between the spin ladders and may lead to the observed continuum in the Raman spectra, as shown in Fig. 4. Thus, we believe that an increased magnetic frustration and fractionalized excitations contribute to and explain the spin-liquid-like

behavior in BLCT. Notably, the observation of a spin-liquid-like state in polycrystalline BLCT is consistent with the recent theoretical report proposing the possibility of realizing such a state even in polycrystalline and amorphous materials [37]. Moreover, we find that the different dopings attempted at the *A/B* site (of $A_2BB'O_6$) in the undoped BCT system drives it to a fully ordered antiferromagnetic state (with Ni doping at the *B* site) due to increased spin interactions, a short-ranged ordered state (with Zn doping at the *B* site) due to broken spin-pair interactions, and a spin-liquid-like state (with La doping at the *A* site) due to a combined contribution from increased frustration along with a broken spin-pair interaction [refer to Figs. 4(c)–4(f) and the Supplemental Material for more details [13]].

In conclusion, a quantum spin-liquid-like state has been realized in chemically modified Ba₂CuTeO₆ upon La doping at the Ba site. Several signatures such as the absence of a spin-glass phase, fermionic density of states in the specific heat, and a broad continuum in the Raman measurement at low and high temperatures were identified to support the existence of the spin-liquid-like state in La-doped Ba₂CuTeO₆. Two approaches are described to explain the origin of the liquid-like correlations, one with an increased magnetic frustration due to lowered Cu-Cu separation in the lattice and the other with an oxidation state conversion of Cu²⁺ into diamagnetic Cu⁺ ions upon La³⁺ doping leading to fractionalized quasiparticles in the system. However, muon spin rotation and relaxation (μ SR) investigations at low temperatures can be useful to ascertain this suggestion which is beyond the scope of the present Letter and can be left for future investigations.

S.S. acknowledges Science and Engineering Research Board (SERB) for funding through ECR/2016/001376 and CRG/2019/002668. Funding from DST-FIST [Project No. SR/FST/PSI-195/2014(C)] and Nano-mission [Project No. SR/NM/NS-84/2016(C)] are also acknowledged. D.N. and A.J. acknowledges support from the CSIR fellowship [09/1020(0139)/2018-EMR-I and 09/1020(0179)/2019-EMR-I]. The authors acknowledge Central Instrumentation Facility at IISER Bhopal for temperature-dependent XRD and SQUID-VSM facilities.

- [1] P. W. Anderson, The resonating valence bond state in La₂CuO₄ and superconductivity, *Science* **235**, 1196 (1987).
- [2] A. Glamazda, P. Lemmens, S.-H. Do, Y. Choi, and K.-Y. Choi, Raman spectroscopic signature of fractionalized excitations in the harmonic-honeycomb iridates β - and γ -Li₂IrO₃, *Nat. Commun.* **7**, 12286 (2016).
- [3] Y. Singh, S. Manni, J. Reuther, T. Berlijn, R. Thomale, W. Ku, S. Trebst, and P. Gegenwart, Relevance of the Heisenberg-Kitaev model for the honeycomb lattice iridates A₂IrO₃, *Phys. Rev. Lett.* **108**, 127203 (2012).
- [4] M.-K. Wu, J. R. Ashburn, C. J. Torng, P.-H. Hor, R. L. Meng, L. Gao, Z. J. Huang, Y. Q. Wang, and C. W. Chu, Superconductivity at 93 K in a new mixed-phase Y-Ba-Cu-O compound system at ambient pressure, *Phys. Rev. Lett.* **58**, 908 (1987).
- [5] A. S. Gibbs, A. Yamamoto, A. N. Yaresko, K. S. Knight, H. Yasuoka, M. Majumder, M. Baenitz, P. J. Saines, J. R. Hester, D. Hashizume, A. Kondo, K. Kindo, and H. Takagi, $S = \frac{1}{2}$ quantum critical spin ladders produced by orbital ordering in Ba₂CuTeO₆, *Phys. Rev. B* **95**, 104428 (2017).
- [6] G. N. Rao, R. Sankar, A. Singh, I. P. Muthuselvam, W. T. Chen, V. N. Singh, G.-Y. Guo, and F. C. Chou, Tellurium-bridged two-leg spin ladder in Ba₂CuTeO₆, *Phys. Rev. B* **93**, 104401 (2016).
- [7] A. Glamazda, Y. S. Choi, S.-H. Do, S. Lee, P. Lemmens, A. N. Ponomaryov, S. A. Zvyagin, J. Wosnitzer, D. P. Sari, I. Watanabe, and K. Y. Choi, Quantum criticality in the coupled two-leg spin ladder Ba₂CuTeO₆, *Phys. Rev. B* **95**, 184430 (2017).

- [8] T. Saha-Dasgupta, The fascinating world of low-dimensional quantum spin systems: *Ab initio* modeling, *Molecules* **26**, 1522 (2021).
- [9] B. Normand and T. M. Rice, Electronic and magnetic structure of $\text{LaCuO}_{2.5}$, *Phys. Rev. B* **54**, 7180 (1996).
- [10] Z. Pan, J. Chen, X. Jiang, L. Hu, R. Yu, H. Yamamoto, T. Ogata, Y. Hattori, F. Guo, X. Fan *et al.*, Colossal volume contraction in strong polar perovskites of $\text{Pb}(\text{Ti}, \text{V})\text{O}_3$, *J. Am. Chem. Soc.* **139**, 14865 (2017).
- [11] J.-M. Tarascon, P. Barboux, P. F. Miceli, L. H. Greene, G. W. Hull, M. Eibschutz, and S. A. Sunshine, Structural and physical properties of the metal (M) substituted $\text{YBa}_2\text{Cu}_{3-x}\text{M}_x\text{O}_{7-y}$ perovskite, *Phys. Rev. B* **37**, 7458 (1988).
- [12] C. Pughe, O. H. Mustonen, A. S. Gibbs, S. Lee, R. Stewart, B. Gade, C. Wang, H. Luetkens, A. Foster, F. C. Coomer *et al.*, Partitioning the two-leg spin ladder in $\text{Ba}_2\text{Cu}_{1-x}\text{Zn}_x\text{TeO}_6$: From magnetic order through spin-freezing to paramagnetism, *Chem. Mater.* **35**, 2752 (2023).
- [13] See Supplemental Material at <http://link.aps.org/supplemental/10.1103/PhysRevB.109.L100405> for details of refined x-ray diffraction data of $\text{Ba}_2\text{CuTeO}_6$ and its La-doped variants, energy-dispersive x-ray spectroscopy, ac magnetic susceptibility, estimation of magnetic moments, magnetic-field-dependent Raman data of $\text{Ba}_2\text{CuTeO}_6$, evolution of magnetic behavior and effect of different dopings, XPS data, and properties of La-doped variants of $\text{Ba}_2\text{CuTeO}_6$.
- [14] M. J. Cliffe and A. L. Goodwin, Pascal: A principal axis strain calculator for thermal expansion and compressibility determination, *J. Appl. Crystallogr.* **45**, 1321 (2012).
- [15] D. Díaz-Anichtchenko, R. Turnbull, E. Bandiello, S. Anzellini, S. N. Achary, and D. Errandonea, Pressure-induced chemical decomposition of copper orthovanadate ($\alpha\text{-Cu}_3\text{V}_2\text{O}_8$), *J. Mater. Chem. C* **9**, 13402 (2021).
- [16] E. Bandiello, P. Rodríguez-Hernández, A. Muñoz, M. B. Buenestado, C. Popescu, and D. Errandonea, Electronic properties and high-pressure behavior of wolframite-type CoWO_4 , *Mater. Adv.* **2**, 5955 (2021).
- [17] D. Tahir and S. Tougaard, Electronic and optical properties of Cu, CuO and Cu_2O studied by electron spectroscopy, *J. Phys.: Condens. Matter* **24**, 175002 (2012).
- [18] T. Böske, K. Maiti, O. Knauff, K. Ruck, M. S. Golden, G. Krabbes, J. Fink, T. Osafune, N. Motoyama, H. Eisaki, and S. Uchida, Cu-O network-dependent core-hole screening in low-dimensional cuprate systems: A high-resolution x-ray photoemission study, *Phys. Rev. B* **57**, 138 (1998).
- [19] N. Pauly, S. Tougaard, and F. Yubero, Determination of the Cu 2p primary excitation spectra for Cu, Cu_2O and CuO, *Surf. Sci.* **620**, 17 (2014).
- [20] O. Mustonen, S. Vasala, E. Sadrollahi, K. Schmidt, C. Baines, H. Walker, I. Terasaki, F. Litterst, E. Baggio-Saitovitch, and M. Karppinen, Spin-liquid-like state in a spin-1/2 square-lattice antiferromagnet perovskite induced by $d^{10}\text{-}d^0$ cation mixing, *Nat. Commun.* **9**, 1085 (2018).
- [21] S. T. Bramwell, M. J. Harris, B. C. den Hertog, M. J. P. Gingras, J. S. Gardner, D. F. McMorrow, A. R. Wildes, A. Cornelius, J. D. M. Champion, R. G. Melko, and T. Fennell, Spin correlations in $\text{Ho}_2\text{Ti}_2\text{O}_7$: A dipolar spin ice system, *Phys. Rev. Lett.* **87**, 047205 (2001).
- [22] J. Laverdière, S. Jandl, A. A. Mukhin, V. Y. Ivanov, V. G. Ivanov, and M. N. Iliev, Spin-phonon coupling in orthorhombic RMnO_3 ($R = \text{Pr}, \text{Nd}, \text{Sm}, \text{Eu}, \text{Gd}, \text{Tb}, \text{Dy}, \text{Ho}, \text{Y}$): A Raman study, *Phys. Rev. B* **73**, 214301 (2006).
- [23] S. Li, Z. Ye, X. Luo, G. Ye, H. H. Kim, B. Yang, S. Tian, C. Li, H. Lei, A. W. Tsen *et al.*, Magnetic-field-induced quantum phase transitions in a van der Waals magnet, *Phys. Rev. X* **10**, 011075 (2020).
- [24] J. Xing, L. D. Sanjeeva, J. Kim, G. R. Stewart, A. Podlesnyak, and A. S. Sefat, Field-induced magnetic transition and spin fluctuations in the quantum spin-liquid candidate CsYbSe_2 , *Phys. Rev. B* **100**, 220407(R) (2019).
- [25] L. Balents, Spin liquids in frustrated magnets, *Nature (London)* **464**, 199 (2010).
- [26] S. Yamashita, T. Yamamoto, Y. Nakazawa, M. Tamura, and R. Kato, Gapless spin liquid of an organic triangular compound evidenced by thermodynamic measurements, *Nat. Commun.* **2**, 275 (2011).
- [27] D. Macdougall, A. S. Gibbs, T. Ying, S. Wessel, H. C. Walker, D. Voneshen, F. Mila, H. Takagi, and R. Coldea, Spin dynamics of coupled spin ladders near quantum criticality in $\text{Ba}_2\text{CuTeO}_6$, *Phys. Rev. B* **98**, 174410 (2018).
- [28] L. J. Sandilands, Y. Tian, K. W. Plumb, Y.-J. Kim, and K. S. Burch, Scattering continuum and possible fractionalized excitations in $\alpha\text{-RuCl}_3$, *Phys. Rev. Lett.* **114**, 147201 (2015).
- [29] K. Y. Choi, Y. G. Pashkevich, V. P. Gnezdilov, G. Guntherodt, A. V. Yermenko, D. A. Nabok, V. I. Kamenev, S. N. Barilo, S. V. Shiryaev, A. G. Soldatov, and P. Lemmens, Orbital fluctuating state in ferromagnetic insulating $\text{LaMnO}_{3+\delta}$ ($0.085 \leq \delta \leq 0.125$) studied using Raman spectroscopy, *Phys. Rev. B* **74**, 064406 (2006).
- [30] K. Jain, S. Lai, and M. V. Klein, Electronic Raman scattering and the metal-insulator transition in doped silicon, *Phys. Rev. B* **13**, 5448 (1976).
- [31] R. Rückamp, E. Benckiser, M. Haverkort, H. Roth, T. Lorenz, A. Freimuth, L. Jongen, A. Möller, G. Meyer, P. Reutler *et al.*, Optical study of orbital excitations in transition-metal oxides, *New J. Phys.* **7**, 144 (2005).
- [32] B. Poojitha, A. Rathore, A. Kumar, and S. Saha, Signatures of magnetostriction and spin-phonon coupling in magneto-electric hexagonal $15R\text{-BaMnO}_3$, *Phys. Rev. B* **102**, 134436 (2020).
- [33] M. Balkanski, R. F. Wallis, and E. Haro, Anharmonic effects in light scattering due to optical phonons in silicon, *Phys. Rev. B* **28**, 1928 (1983).
- [34] S. Saha, D. V. S. Muthu, S. Singh, B. Dkhil, R. Suryanarayanan, G. Dhalenne, H. K. Poswal, S. Karmakar, S. M. Sharma, A. K. Revcolevschi, and A. K. Sood, Low-temperature and high-pressure raman and x-ray studies of pyrochlore $\text{Tb}_2\text{Ti}_2\text{O}_7$: Phonon anomalies and possible phase transition, *Phys. Rev. B* **79**, 134112 (2009).
- [35] S. Pal, A. Seth, P. Sakrikar, A. Ali, S. Bhattacharjee, D. V. S. Muthu, Y. Singh, and A. K. Sood, Probing signatures of fractionalization in the candidate quantum spin liquid Cu_2IrO_3 via anomalous Raman scattering, *Phys. Rev. B* **104**, 184420 (2021).
- [36] K. Momma and F. Izumi, VESTA 3 for three-dimensional visualization of crystal, volumetric and morphology data, *J. Appl. Crystallogr.* **44**, 1272 (2011).
- [37] A. G. Grushin and C. Repellin, Amorphous and polycrystalline routes toward a chiral spin liquid, *Phys. Rev. Lett.* **130**, 186702 (2023).